

Article

Optimization of Shingled-Type Lightweight Glass-Free Solar Modules for Building Integrated Photovoltaics

Min-Joon Park ¹ , Sungmin Youn ¹, Kiseok Jeon ¹, Soo Ho Lee ² and Chaehwan Jeong ^{1,*}

¹ Green Energy & Nano Technology R&D Group, Korea Institute of Industrial Technology, Gwangju 61012, Korea; pk5659@kitech.re.kr (M.-J.P.); aslove1@kitech.re.kr (S.Y.); jks8287@kitech.re.kr (K.J.)

² Photovoltaic R&D Center, Solbigtech Co., Ltd., Gwangju 61012, Korea; leesh@solbig-tech.com

* Correspondence: chjeong@kitech.re.kr

Abstract: High-power and lightweight photovoltaic (PV) modules are suitable for building-integrated photovoltaic (BIPV) systems. Due to the characteristics of the installation sites, the BIPV solar modules are limited by weight and installation area. In this study, we fabricated glass-free and shingled-type PV modules with an area of 1040 mm × 965 mm, which provide more conversion power compared to conventional PV modules at the same installed area. Further, we employed an ethylene tetrafluoroethylene sheet instead of a front cover glass and added an Al honeycomb sandwich structure to enhance the mechanical stability of lightweight PV modules. To optimize the conversion power of the PV module, we adjusted the amount of dispensed electrically conductive adhesives between the solar cells. Finally, we achieved a conversion power of 195.84 W at an area of 1.004 m², and we performed standard reliability tests using a PV module that weighed only 9 kg/m².

Keywords: lightweight photovoltaic modules; shingled-type strings; ethylene tetrafluoroethylene; Al honeycomb structures; building integrated photovoltaics



Citation: Park, M.-J.; Youn, S.; Jeon, K.; Lee, S.H.; Jeong, C. Optimization of Shingled-Type Lightweight Glass-Free Solar Modules for Building Integrated Photovoltaics. *Appl. Sci.* **2022**, *12*, 5011. <https://doi.org/10.3390/app12105011>

Academic Editor: Fabrice Goubard

Received: 19 April 2022

Accepted: 13 May 2022

Published: 16 May 2022

Publisher's Note: MDPI stays neutral with regard to jurisdictional claims in published maps and institutional affiliations.



Copyright: © 2022 by the authors. Licensee MDPI, Basel, Switzerland. This article is an open access article distributed under the terms and conditions of the Creative Commons Attribution (CC BY) license (<https://creativecommons.org/licenses/by/4.0/>).

1. Introduction

Renewable energy generation technologies have been continuously developed owing to concerns related to the environment and energy independence. The rapid growth of photovoltaic (PV) technology compared to other renewables has led to numerous studies on this topic [1,2]. As part of these studies, building-integrated photovoltaic (BIPV) systems play an essential role in generating electricity [3]. Recently, the BIPV market has been estimated to grow by approximately 40% per year from 2018 to 2026 [4]. In the case of BIPV, there are two limiting factors regarding the weight and installation area of the module to be installed [1,2]. To solve these problems, it is necessary to study the design of high-power and lightweight c-Si PV modules for BIPV systems.

Generally, glass is most commonly used for the front and rear covers in BIPV because it is a highly transparent, mechanically stable, and sustainable material that is familiar within the building industry. However, the weight of conventional PV modules with c-Si solar cells, ranging from 12 to 16 kg/m² for glass-backsheet modules and from 16 to 20 kg/m² for glass-glass modules, limits their usage on roofs or facades of buildings [5,6]. Modules with a non-glass cover include a polymer such as ethylene tetrafluoroethylene copolymer (ETFE), polyamide (PA), polypropylene (PP), polyethylene terephthalate (PET), and polyvinyl fluoride (PVF), which are typically used for lightweight applications such as roofs and facades of buildings [7–10]. Although the lightweight PV module is very attractive, it is not yet applicable to BIPV owing to reliability and low module stiffness issues. The thin polymer sheet used to substitute the glass does not completely protect the solar cells owing to its low mechanical stability.

Recently, many researchers have investigated the enhancement of the mechanical stability of lightweight PV modules for BIPV systems [7,10–13]. Martins et al. employed

an Al honeycomb sandwich structure at the rear of lightweight and mechanically stable c-Si PV modules [12,13]. This glass-free and lightweight PV module architecture exhibited enhanced mechanical stability and reliability. However, conversion power enhancement of lightweight PV modules for BIPV systems has not yet been studied. In this study, we combined a shingled-type PV design for high-power conversion and glass-free lightweight module with an Al honeycomb sandwich structure on the rear side. The shingled-type c-Si PV module has a larger active area compared to the conventional PV module [14–18]. Because serially connected shingled-type strings do not have a busbar electrode on the front side this design increases the module power for the same installed area used in conventional PV modules. In our previous work, we fabricated an 1100 mm × 1980 mm shingled-type c-Si PV module and performed conversion power and standard reliability tests [15]. Based on the combination of a shingled-type design and an Al honeycomb sandwich structure, we fabricated a high-power, lightweight c-Si PV module and analyzed the electrical properties and reliability of the PV modules.

2. Materials and Methods

Figure 1 shows a schematic of the shingled cell-to-string fabrication process. To prepare the separated cells, we divided a M2-size c-Si solar cell (156.85 mm × 156.85 mm, Shingled patterned p-PERC cell, Shinsung E&G, Seongnam, Korea) into five equal pieces to make a shingled string using the laser scribing process. We scribed the solar cells using a nanosecond laser (532 nm, 50 kHz, 20 ns, 10 W, Coherent, Santa Clara, CA, USA) and then broke them mechanically. The separated cells were assembled using electrically conductive adhesives (ECA, XCA-8311, Hankel, Dusseldorf, Germany). We dispensed the ECA on top of the front busbar electrode and connected the back electrode of the next separated cell to create a shingled string structure. An ECA curing temperature of 140 °C was used to assemble the separated cells.

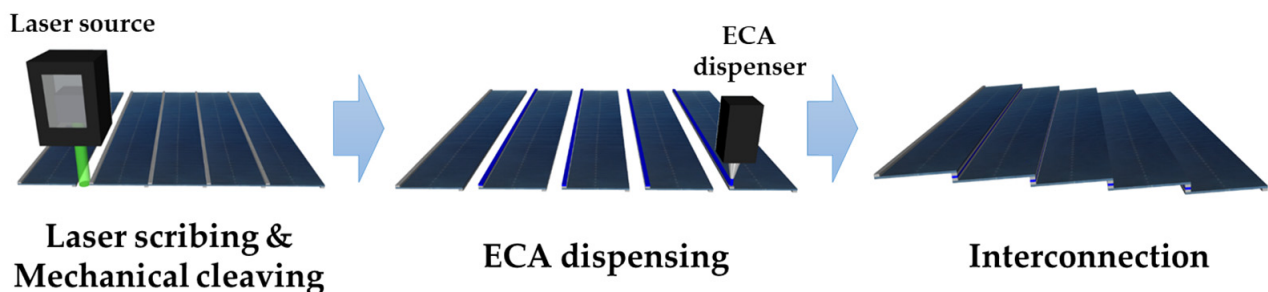


Figure 1. Schematic of the shingled-type cell-to-string structures and fabrication process.

Figure 2 shows a schematic of the shingled-type lightweight glass-free solar module for BIPV applications with a description of all the constituent layers. We used ETFE (150 µm, Jolywood, Suzhou, China) film as the front sheet and ethylene-vinyl acetate (EVA, 450 µm, SVECK, Jiangsu, China) as adhesives. The Al honeycomb sandwich structure was fabricated using glass fiber-reinforced plastic (FRP, FR-4, Keunying industrial, Seoul, Korea)/Al honeycomb core (10 mm, Hongseong Industrial, Seoul, Korea)/Al plate (1 mm, POSCO, Pohang, Korea) with EVA adhesives. We used a lamination system (BSL2222OC, Boostsolar, Qinhuangdao, China) to laminate the shingled-type PV module with an Al honeycomb sandwich structure at 140 °C for 660 s. An electroluminescence (EL) system (Portable EL, 600 W, TNE TECH, Cheongju, Korea) was used to analyze the damage to the shingled strings and modules. The PV cells and modules were measured using a solar simulator (WXS-1555-L2, WACOM, Gajo, Japan) and an I-V analyzer (DKSCT-3T, DENKEN, Yufu, Japan) for AM 1.5 G (100 mW/m²) illumination. For the reliability test of the PV modules, we performed a temperature cycle 200 test (TC 200, SEC-4100, ALISTA, Victoria, Australia), damp heat 1000 tests (DH 1000, condensing chamber, ALISTA), mechanical load 2400 tests (ML 2400) in IEC 61215 standards. In the TC 200 test, we applied the maximum power current between −40 °C and 85 °C and repeated 200 cycles with a

constant temperature change to measure the power reduction rate. In the DH 1000 test, we measured the power reduction rate before and after the test after 1000 h in an environment of a temperature of 85 °C and a relative humidity of 85%. In the ML 2400 test, we measured the power reduction rate before and after the test after applying a load with 2400 Pa on the front and rear of the module.

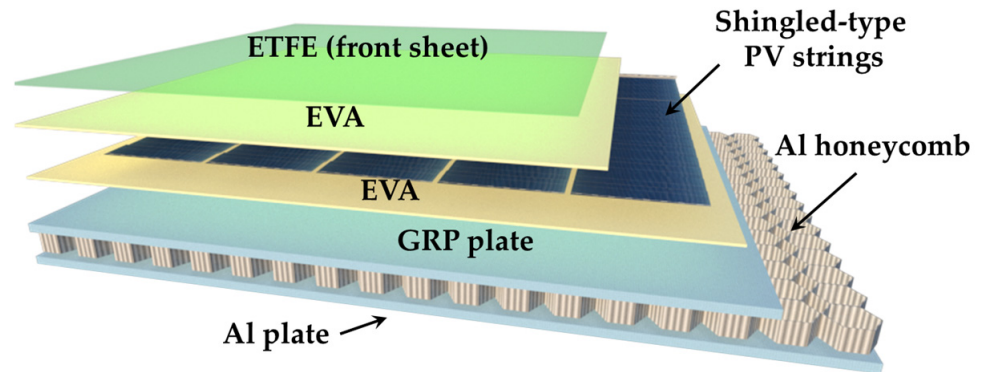


Figure 2. Schematic of the shingled-type lightweight glass-free solar module.

3. Results & Discussion

The images in Figure 3a depict the front and rear of the separated cells obtained using laser scribing. Figure 3b shows the conversion power (P_M) distribution of 20 separated cells. The average P_M of the separated cells was 1.014 ± 0.01 W. The inset of Figure 3b shows the I-V curve of a champion cell. The value of the P_M decreased about 1.7% compared to the value of the P_M without electrical losses. This phenomenon is expected to reduce the P_M due to laser scribing damage [15]. To minimize P_M loss, we will optimize the laser scribing process. Next, we fabricated 17 connected shingled strings using the ECA dispensing and curing process. Because of the top of the front busbar electrode and the back electrode of the next separated cell, there is no busbar electrode on the top of the shingled string, as shown in Figure 4a. Therefore, shingled-type PV modules exhibit a larger P_M than conventional PV modules in the same installation area. To analyze the damage to the shingled strings, we measured the EL images with an applied current injection of 0.9 A in Figure 4b. The EL image shows the absence of critical cracks and damage in the interconnection process.

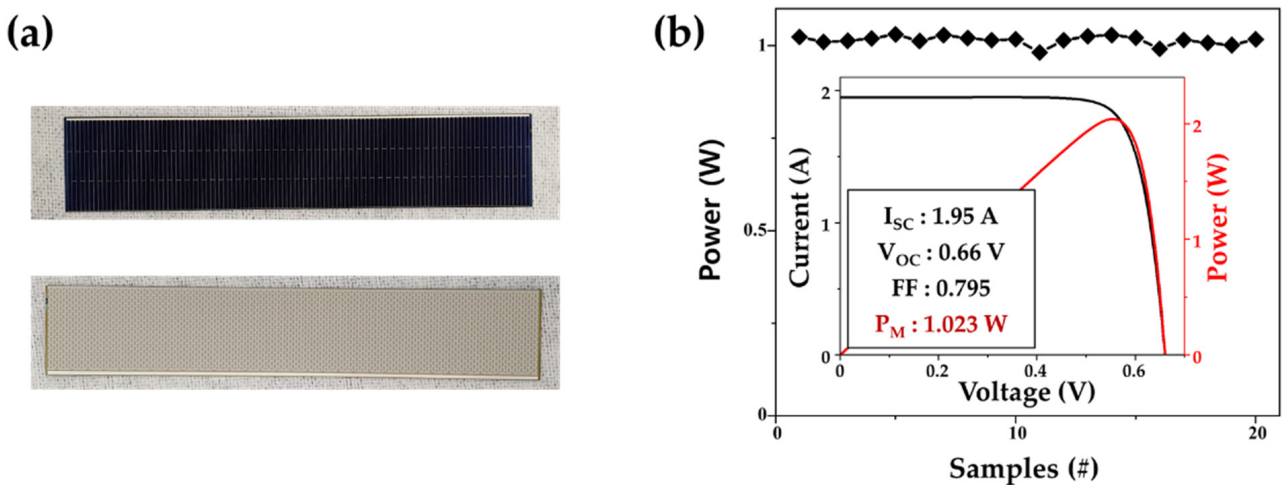


Figure 3. (a) Photo images of the front and rear sides of the separated cells and (b) the conversion power distribution of 20 separated cells. Inset: I-V curve of a champion cell.

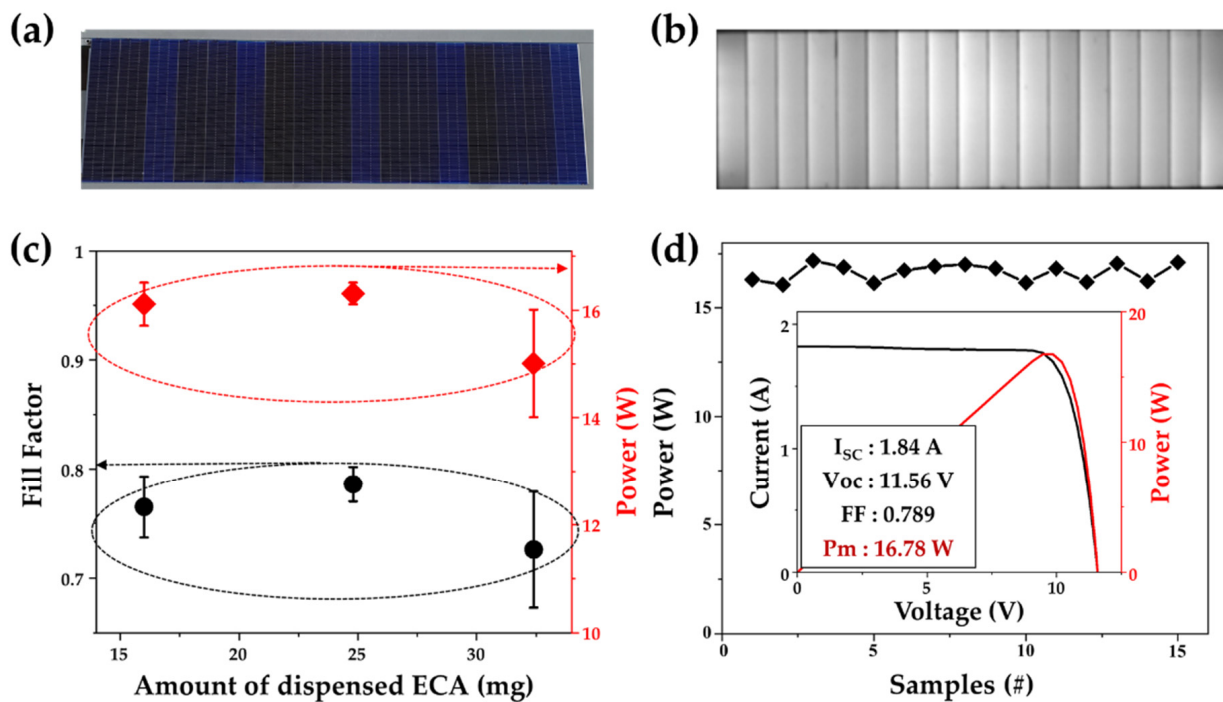


Figure 4. (a) Photographic and (b) electroluminescence images of shingled-type strings. (c) Fill factors and conversion powers with varying amounts of dispensed ECA. (d) P_M distribution of 15 shingled-type strings. Inset: I-V curve of a shingled-type string.

To optimize the conversion power of the shingled-type strings, we adjusted the amount of dispensed ECA. In our previous work, a 0.17 mm overlap width between the top and bottom separated cells for the interconnection was found to yield the best P_M [15]. The amount of dispensed ECA was adjusted by the rounds per minute (RPM) control of the dispenser to optimize the P_M of the strings. When the RPM of the dispenser was 100, 120, and 140, the dispensed amounts of ECA were 16, 24.8, and 32.4 mg, respectively. We found that the fill factor and P_M values of the string were optimized when the dispensed amount of ECA was 24.8 mg in Figure 4c. The cells interconnected with ECA formed a circuit in which two shingle-diode models representing the separated cell were connected in series [19]. Consequently, the serial resistance of the ECA interconnection was added to the shingled strings, making it a critical factor for optimizing the P_M . Figure 4d shows the P_M distribution of 15 shingled-type strings. The average P_M of shingled-type strings was 16.64 ± 0.57 W. The inset of Figure 4d shows the I-V curve of a shingled-type string. Compare with the I-V curve of separated cell in Figure 3b, the value of short circuit current (I_{SC}) and fill factor (FF) decreased by approximately 0.11 A and 0.009. The value of the P_M decreased about 4.5% compared to the value of the P_M without electrical and optical losses. In case of conventional PV modules with metallic wire interconnections, the P_M reduction rate is about 4.8% [20].

We fabricated a 1040 mm \times 965 mm shingled-type PV module with an Al honeycomb structure using 17 interconnected strings, as shown in Figure 5a. We measured EL images with an applied current injection of 3 A to analyze the damage to the PV module, as shown in Figure 5b. The EL image demonstrates the absence of critical cracks or damages during the fabrication of the shingle-type PV module with an Al honeycomb structure. Figure 5c shows the I-V curves of the shingle-type PV module. We achieved a P_M of 195.84 W at an area of 1.004 m² and solar-to-power conversion efficiency of 19.5% for the best PV module. In our shingled-type PV module, we used 12 string arrays with 204 pieces of separated cells. In the 1 m² area, we integrated approximately 40.8 M2-size Si solar cells, i.e., 4.8 solar cells more than a conventional PV module. Moreover, the weight of the PV

module with the Al honeycomb structure was only 9 kg/m², which is 25% lighter than that of the glass-backsheet PV module.

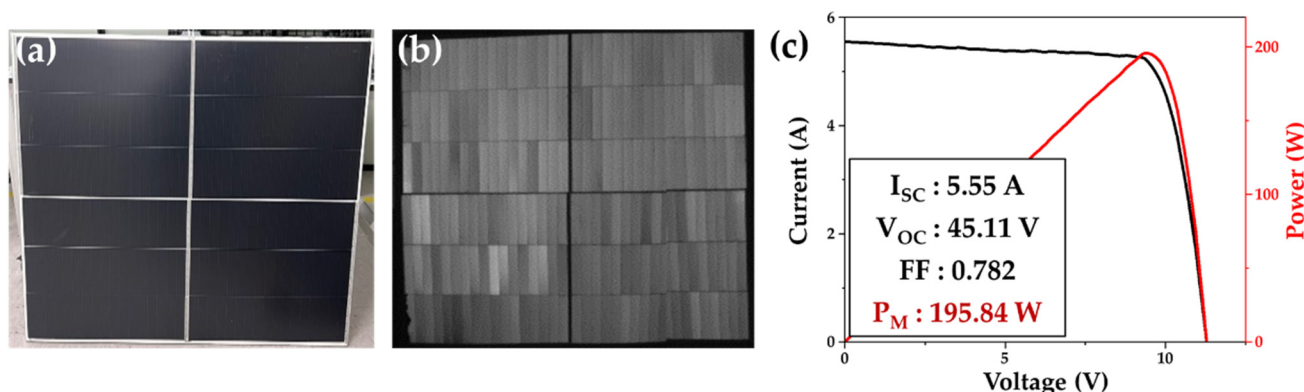


Figure 5. (a) Photograph, (b) electroluminescence images, and (c) I-V curve of the shingled-type lightweight PV module.

Finally, we performed ML 2400, DH 1000, and TC 200 for standard reliability tests of lightweight shingled-type PV modules under IEC 61215. We verified the durability of the fabricated lightweight shingled-type PV modules from these tests. Table 1 shows the changes in module performance before and after the standard reliability tests. After ML 2400, we confirmed that the decrease in the FF value was the cause of the reduction of the conversion power of the PV module. This result shows a phenomenon caused by cracks or damage occurring during the ML test [21].

Table 1. Result of standard reliability tests of lightweight shingled-type PV modules under IEC 61215 viz. mechanical load 2400, damp heat 1000 and temperature cycling 200 tests.

	ML 2400		DH 1000		TC 200	
	Before Test	After Test	Before Test	After Test	Before Test	After Test
V _{OC} (V)	21.50	21.49	21.63	21.59	21.79	21.76
I _{SC} (A)	10.71	10.74	10.99	10.84	11.04	10.88
FF	0.717	0.706	0.748	0.744	0.753	0.743
P _M (W)	165.09	162.88	177.78	174.23	181.14	175.78
P _M loss		1.34%		2.00%		2.96%

On the other hand, the I_{SC} value decreases after the DH 1000 and TC 200 tests. The mechanisms for degradation of conversion power during damp heat exposure are attributed as follows: (1) delamination among the encapsulation polymer and the solar cells or front/back covers due to adhesion loss, (2) grid corrosion due to the by-product such as acetic acid. Moisture is well known to cause problems with polymers and adhesions. Unfortunately, EVA has a high moisture absorption rate and poor stability in a humid environment [22]. Moreover, absorbed moisture by EVA adhesive can generate a by-product of acetic acid and increase the series resistance due to grid corrosion [23]. The decrease in the I_{SC} value after the TC 200 test was caused by discoloration of PV module. Wohlgenuth et al. analyzed the I-V measurement after conducting the thermal cycling test, and found that P_M decreased due to the decrease of I_{SC} [24]. They concluded that transmittance decreases due to the change in color of EVA after thermal cycling, resulting in a decrease in current. In the result, the reductions in the conversion powers of the lightweight shingled-type PV modules were less than five percent after the standard reliability tests.

4. Conclusions

In summary, we fabricated a lightweight shingled-type PV module with an ETFE front sheet and an Al honeycomb structure. The ETFE film replaced the front cover glass

to reduce the module weight, and an Al honeycomb structure was used instead of the front glass to improve the mechanical rigidity. To enhance the P_M of the PV module, we integrated 12 string arrays with 40.8 M2-size Si solar cells. In our lightweight shingled-type PV module, 4.8 M2-size Si solar cells were more integrated compared to the optimized conventional PV module at the same area. Moreover, we adjusted the amount of dispensed ECA to optimize its performance. The lightweight shingled-type PV module had a P_M of 195.84 W at a 1.004 m² area and weighed only 9 kg/m². Finally, we performed standard reliability tests to verify the durability of lightweight shingled-type PV modules. The conversion power reduction of the PV modules were less than five percent.

Author Contributions: Conceptualization, M.-J.P.; methodology, M.-J.P. and S.Y.; data curation, M.-J.P., S.H.L. and K.J. writing—original draft preparation, M.-J.P.; writing—review and editing, M.-J.P. and C.J.; supervision, C.J. All authors have read and agreed to the published version of the manuscript.

Funding: This work was supported by the International Energy Joint R&D Program of the Korea Institute of Energy Technology Evaluation and Planning (KETEP). The authors also acknowledge financial resources granted by the Ministry of Trade, Industry & Energy, Republic of Korea. (No. 20203030010200).

Institutional Review Board Statement: Not applicable.

Informed Consent Statement: Not applicable.

Data Availability Statement: Not applicable.

Conflicts of Interest: The authors declare no conflict of interest.

References

- Kuhn, E.T.; Erban, C.; Heinrich, M.; Eisenlohr, J.; Ensslen, F.; Neuhaus, D.H. Review of technological design options for building integrated photovoltaics (BIPV). *Energy Build.* **2021**, *231*, 110381. [[CrossRef](#)]
- Biyik, E.; Araz, M.; Hepbasli, A.; Shahrestani, M.; Yao, R.; Shao, L.; Essah, E.; Oliveira, A.C.; Caño, T.; Rico, E.; et al. A key review of building integrated photovoltaic (BIPV) systems. *Eng. Sci. Technol. Int. J.* **2017**, *20*, 833–858. [[CrossRef](#)]
- Li, C.; Wang, R.Z. Building integrated energy storage opportunities in China. *Renew. Sustain. Energy Rev.* **2012**, *16*, 6191–6211. [[CrossRef](#)]
- Ballif, C.; Perret-Aebi, L.; Lufkin, S.; Rey, E. Integrated thinking for photovoltaics in buildings. *Nat. Energy* **2018**, *3*, 438–442. [[CrossRef](#)]
- Reese, M.O.; Glynn, S.; Kempe, M.D.; McGott, D.L.; Dabney, M.S.; Barnes, T.M.; Booth, S.; Feldman, D.; Haegel, N.M. Increasing markets and decreasing package weight for high-specific-power photovoltaics. *Nat. Energy* **2018**, *3*, 1002–1012. [[CrossRef](#)]
- Nussbaumer, H.; Klenk, M.; Keller, N. Small unit compound modules: A new approach for light weight PV modules. In Proceedings of the 32nd European Photovoltaic Solar Energy Conference and Exhibition, Munich, Germany, 20–24 June 2016; pp. 56–60.
- Bittmann, E.; Mayer, O.; Zettl, M.; Stern, O. Low Concentration PV with Polycarbonate. In Proceedings of the 23rd European Photovoltaic Solar Energy Conference and Exhibition, Valencia, Spain, 1–5 September 2018; pp. 537–539.
- Drabczyk, K.; Sobik, P.; Starowicz, Z.; Gawlińska, K.; Pluta, A.; Drabczyk, B. Study of lamination quality of solar modules with PMMA front layer. *Microelectron. Int.* **2019**, *36*, 100–103. [[CrossRef](#)]
- Oreski, G.; Eder, G.C.; Voronko, Y.; Omazic, A.; Neumaier, L.; Mühleisen, W.; Ujvari, G.; Ebner, R.; Edler, M. Performance of PV modules using co-extruded backsheets based on polypropylene. *Sol. Energy Mater. Sol. Cells* **2021**, *223*, 110976. [[CrossRef](#)]
- Kajisa, T.; Miyachi, H.; Mizuhara, K.; Hayashi, H.; Tokimitsu, T.; Inoue, M.; Hara, K.; Masuda, A. Novel lighter weight crystalline silicon photovoltaic module using acrylic-film as a cover sheet. *Jpn. J. Appl. Phys.* **2014**, *53*, 092302. [[CrossRef](#)]
- Nussbaumer, H.; Klenk, M.; Keller, N.; Ammann, P.; Thurnheer, J. Record-light weight c-Si modules based on the small unit compound approach mechanical load tests and general results. In Proceedings of the 33rd European Photovoltaic Solar Energy Conference and Exhibition, Amsterdam, The Netherlands, 25–29 September 2017; pp. 146–150.
- Martins, A.C.; Chapuis, V.; Sculati-Meillaud, F.; Virtuani, A.; Ballif, C. Light and durable: Composite structures for building-integrated photovoltaic modules. *Prog. Photovolt. Res. Appl.* **2018**, *26*, 718–729. [[CrossRef](#)]
- Martins, A.C.; Chapuis, V.; Virtuani, A.; Li, H.; Perret-Aebi, L.; Ballif, C. Thermo-mechanical stability of lightweight glass-free photovoltaic modules based on a composite substrate. *Sol. Energy Mater. Sol. Cells* **2018**, *187*, 82–90. [[CrossRef](#)]
- Dickson, D.C.; Heights, P. Photo-Voltaic Semiconductor Apparatus or the Like. U.S. Patent 2938938, 31 May 1960.
- Park, M.; Song, J.; Jee, H.; Moon, D.; Jeong, C.; Jee, H. Improvement in the power of shingled-type photovoltaic module by control of the overlapped width. *J. Korean Phys. Soc.* **2020**, *77*, 1040–1043. [[CrossRef](#)]

16. Springer, M.; Bosco, N. Linear viscoelastic characterization of electrically conductive adhesives used as interconnect in photovoltaic modules. *Prog. Photovolt. Res. Appl.* **2020**, *28*, 659–681. [[CrossRef](#)]
17. Jee, H.; Lee, S.; Jeong, C.; Lee, J. Electrically conductive adhesives and the shingled array cell for high density modules. *J. Nanosci. Nanotechnol.* **2019**, *19*, 1360–1363. [[CrossRef](#)] [[PubMed](#)]
18. Rabanal-Arabach, J.; Rudolph, D.; Ullmann, I.; Halm, A.; Schneider, A.; Fischer, T. Cell-to-module conversion loss simulation for shingled-cell concept. In Proceedings of the 33rd European Photovoltaic Solar Energy Conference and Exhibition, Amsterdam, The Netherlands, 25–29 September 2017; pp. 178–182.
19. Park, J.; Oh, W.; Park, H.; Jeong, C.; Choi, B.; Lee, J. Analysis of solar cells interconnected by electrically conductive adhesives for high-density photovoltaic modules. *Appl. Surf. Sci.* **2019**, *484*, 732–739. [[CrossRef](#)]
20. Haedrich, I.; Eitner, U.; Wiese, M.; Wirth, H. Unified methodology for determining CTM ratios: Systematic prediction of module power. *Sol. Energy Mater. Sol. Cells* **2014**, *131*, 14–23. [[CrossRef](#)]
21. Wohlgemuth, J.H.; Kurtz, S. Reliability testing beyond qualification as a key component in photovoltaic's progress toward grid parity. In Proceedings of the 2011 IEEE International Reliability Physics Symposium, Monterey, CA, USA, 10–14 April 2011; pp. 5E.3.1–5E.3.6.
22. McIntosh, K.R.; Powell, N.E.; Norris, A.W.; Cotsell, J.N.; Ketola, B.M. The effect of damp-heat and UV aging tests on the optical properties of silicone and EVA encapsulants. *Prog. Photovolt. Res. Appl.* **2011**, *19*, 294–300.
23. Shi, X.-M.; Zhang, J.; Li, D.-R.; Chen, S.J. Effect of damp-heat aging on the structures and properties of ethylene-vinyl acetate copolymers with different vinyl acetate contents. *J. Appl. Polym. Sci.* **2009**, *112*, 2358–2365. [[CrossRef](#)]
24. Wohlgemuth, J.H.; Petersen, R.C. Reliability of EVA modules. In Proceedings of the 23th IEEE Photovoltaic Specialists Conference, Louisville, KY, USA, 10–14 May 1993; pp. 1090–1094.